Photoactivation dynamics in photosynthetic and signal transduction proteins studied by ultra-fast time-resolved spectroscopy

Bonetti, C.

2009

document version
Publisher's PDF, also known as Version of record

Chapter 6 The role of key amino acids in the photoactivation pathway of the *Synechocystis* Slr1694 BLUF domain

Abbreviations: BLUF, Blue Light photoreceptors Using FAD; FAD, Flavin Adenine Dinucleotide; FMN, Flavin Mono-Nucleotide; Y: Tyrosine; W, Tryptophan; Q, Glutamine; N, Asparagine; S, Serine; M, Methionine; I, Isoleucine; A, Alanine; FTIR, Furier Transform Infra-Red ; *Escherichia coli* (*E.coli*); USP, Ultra Short Pulse, FWHM, Full, Width at Half Maximum; EADS, Evolution-Associated Difference Spectra; SADS, Species-Associated Difference Spectra; WT, Wild Type; RMS, Root Mean Square Error; (RMS); FAD^*, FAD Excited State; $FADH^\bullet$, neutral FAD semiquinone; $FAD^{\bullet-}$, FAD anionic semiquinone; $W^{\bullet+}$, tryptophan radical cation, $W^\bullet$, tryptophan neutral radical; KIE, Kinetic Isotope Effect.

Abstract

BLUF (blue light sensing using FAD) domains belong to a novel group of blue light sensing receptor proteins found in microorganisms. The role of specific aromatic and polar residues in the direct vicinity of FAD, Y8, W91 and S28 in Slr1694 BLUF protein of *Synechocystis* was investigated using

Bonetti C., Stierl M., Mathes T., van Stokkum I. H. M., Mullen K. M., Cohen-Stuart T. A. , van Grondelle R., Hegemann P. and John T.M. Kennis

mutants with substitution Y8W, W91F and S28A. The W91F and S28A mutants formed the red-shifted signaling state upon blue-light illumination, whereas in the Y8W mutant, signaling state formation was abolished. The W91F mutant shows photoactivation dynamics that involve the successive formation of an FAD anionic and neutral semiquinone radical on a picosecond timescale, followed by radical-pair recombination to result in the long-lived signaling state in less than 100 ps. The photoactivation dynamics and quantum yield of signaling state formation were essentially identical to those of wild type, indicating that W91 does hardly or not at all participate in the Slr1694 primary photochemistry. Thus, only one significant light-driven electron transfer pathway is available in Slr1694, involving electron transfer from Y8 to FAD. In the S28A mutant, the photoactivation dynamics was essentially the same as in wild type as well, although due to a limited signal-to-noise only a neutral semiquinone $FADH^{\bullet}$ intermediate was detected en route to the red-shifted signaling state. The signaling state quantum yield and dark recovery rate were comparable with wild type. Thus, S28 does not play an essential role in the initial hydrogen-bond switching reaction in Slr1694 beyond its influence on the absorption spectrum. In the Y8W mutant, two deactivation branches upon excitation were identified: the first involves a neutral semiquinone $FADH^{\bullet}$ that was formed in ~1 ps and recombines in 10 ps and is tentatively assigned to a $FADH^{\bullet}$ - $W8^{\bullet}$ radical pair. The second deactivation branch forms $FADH^{\bullet}$ in 8 ps and evolves to $FAD^{\bullet-}$ in 200 ps, which recombines to the ground state in about 3 ns. In the latter branch, W91 is tentatively assigned as the FAD redox partner. Overall, the results are consistent with a photoactivation mechanism for BLUF domains where signaling state formation proceeds via light-driven electron and proton transfer from Y8 to FAD, followed by a hydrogen-bond rearrangement and radical-pair recombination.

Introduction

Blue light photoreceptors using flavin cofactors have been the focus of recent research because of their novel mechanisms of photoactivation in contrast to “classical” photoreceptors like phytochromes and rhodopsins. Especially members of the BLUF (Blue Light photoreceptors Using FAD) family [1-3] show an especially intriguing light-induced

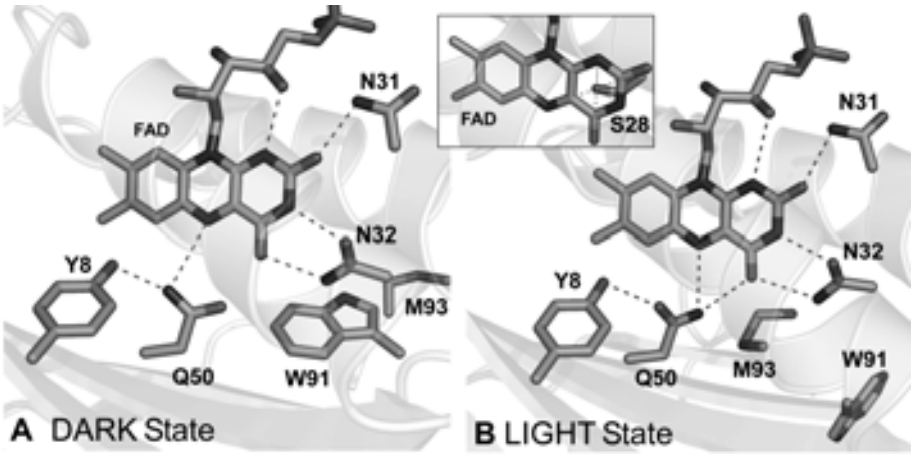

Figure 1: Three-dimensional structure of the Synechocystis Slr1694 BLUF domain in its proposed dark (**A**) and light (**B**) states. Conserved tyrosine (Y8), glutamine (Q50) and asparagine (N32) side chains are involved in an intricate hydrogen-bond network with flavin.

proton network rearrangement resulting in a 10-15 nm red-shifted spectrum of the signaling state. The BLUF domain shows a ferredoxin-like fold consisting of a five-stranded β-sheet with two α-helices packed on one side of the sheet, with the isoalloxazine ring of flavin adenine dinucleotide (FAD) positioned between the two α -helices [4-7]. FAD is noncovalently bound to the protein through a number of hydrogen bonds and hydrophobic interactions. Figure 1 shows the three-dimensional structure of the *Synechocystis* Slr1694 BLUF domain in its proposed dark and light states, with the FAD binding pocket highlighted [7]. Conserved tyrosine (Y8), glutamine (Q50) and asparagine (N32) side chains are involved in an intricate hydrogen-bond network with flavin. The molecular identities of the BLUF dark- and photoactivated states remain controversial as X-ray and NMR structures have given different orientations for the conserved glutamine in the dark (i.e. with the amino group hydrogen bonded to the conserved tyrosine or to FAD C_4=O, see Figure 1A and B). A similar issue holds for W91 and M93, which were found either close to FAD or exposed to the solvent [4-8].

The current opinion on the photoactivation of the BLUF domains as observed by steady state FTIR [9, 10] , Raman [11, 12] and ultrafast visible and IR spectroscopy [13-18] includes light-induced radical pair formation by electron and proton transfer from an essential tyrosine side-chain (Y8) to the flavin cofactor on the picosecond timescale.

Subsequently, hydrogen bond rearrangement takes place, possibly involving ~180 ° rotation of the amide group of an essential glutamine sidechain (Q50) which is followed by radical-pair recombination in less than 100 ps. The resulting reoxidized flavin forms a hydrogen-bond switched network in the flavin binding pocket.

Although Y8 has been experimentally shown to be essential for electron transfer, it is not certain whether the proton is also transferred from this residue. Also, the mode of signal transduction in BLUF domains is essentially unknown since structural changes are mainly limited to the side chains in the immediate vicinity of FAD and no obvious propagation to the surface has been demonstrated. So far, only a possibly light-induced displacement of the semiconserved W104 in AppA by the conserved M106 and the concomitant backbone rearrangement is a possible candidate for signal transduction as implicated by crystal structures [6, 7, 19], spectroscopy [19], and physiological observations [20]. The backbone rearrangement might affect the oligomerisation state of a recently proposed oligomeric BLUF/effector complex and thereby transduce the biological signal [21].

One major problem in understanding the nature of the primary intermediates is the heterogenity of the ground state in BLUF domains which leads to a complicated transient behavior after light excitation [22]. The data recorded by ultrafast spectroscopy therefore has to be analyzed by modeling the reaction using a procedure called target analysis [23]. To simplify the analysis it would be feasible to stabilize the intermediates so they can be studied under steady-state(-like) conditions. Another aspect in the study of BLUF photoreceptors is their rather large variety in their transient behavior. Despite their high sequence homology the signaling state lifetime of BLUF domains varies from Slr1694, BlrB [5], Tll0078 [24] with around 10s, to AppA [22] and YcgF [25] with 50-100 fold slower decay times.

In the AppA BLUF domain it was shown that the semi-conserved tryptophan in the vicinity of FAD (W104) also contributes to electron transfer to the flavin [15]. The latter observation lended support to the 'W-in' conformation of W104 in dark-state AppA. Tryptophan at this position is conserved in 85% of the BLUF domain family.

One interesting candidate which might explain the diverse behavior in BLUF-domains might be S28 in Slr1694. Serine is conserved at this position in 43% of the BLUF domain family. S28 is a polar, acidic residue

in close vicinity to FAD. The hydroxyl group of this serine introduces a dipolar interaction with the heteroatoms of the flavin and therefore alters the spectroscopic properties of the protein and possibly also the dynamics after light excitation. Recent quantum mechanical studies on AppA [26] proposed an essential role of this residue (S41) for the theoretical description of the red shifted spectrum of the light activated state. Moreover, in the calculations, S41 was found to switch conformation in concert with W104 upon light absorption. It is thus of interest to study the photodynamics of the S28A mutant of Slr1694.

It was shown previously that the conserved tyrosine (Y8 in Slr1694, Y21 in AppA) is essential for BLUF photoactivation by acting as the electron donor and hydrogen-bond donor/acceptor of the conserved glutamine [13, 15, 24, 27, 28]. It is known that besides tyrosine, tryptophan can act as an efficient electron donor to flavin. For AppA, removal of Y21 by site-directed mutagenesis leads to redundant electron transfer processes from W104 which result in short-lived FAD-W radical pairs, but not in a stable photoproduct [14, 15]. The question then arises whether W can take up some of the roles of the conserved Y in BLUF domains, i.e., electron transfer and hydrogen-bond switch capabilities. For this reason we constructed the Y8W mutant of Slr1694.

In this work we studied the role of these (semi-)conserved amino acid side chains in the vicinity of the flavin in Slr1694 by ultrafast visible spectroscopy on mutated proteins with respect to their role in electron/proton transfer during the primary processes.

Materials and Methods

Sample preparation

Mutations were introduced into pET28a(+)-slr1694 [16, 29] by site-directed mutagenesis (Quikchange ® , Stratagene) using the primers in Table 1. The mutated DNA was confirmed by sequence analysis. Proteins were expressed in *Escherichia coli* (*E.coli*) strain BL21(DE3)pLysS over night at 18 ° C in the presence of 0.7 mM IPTG and purified as described before [13].

Table 1: Oligonucleotides used for site-directed mutagenesis. The mismatched bases are printed bold.

Oligonucleotide	Sequence (5' → 3')
Y8W_fw	GTTTGTACCGTTTGATTT**GG**AGCAGTCAGGGCATTCCC
Y8W_rv	GGGAATGCCCTGACTGCT**CC**AAATCAAACGGTACAAAC
Slr_S28A_fw	GATATCTTAGAATCT**G**CCCAAAGAAATAATCCGGC
Slr_S28A_rv	GCCGGATTATTTCTTTGGG**C**AGATTCTAAGATATC
Slr_W90F	GAAGAAACTTCGAGGTTT**TC**TCTATGCAAGCGATC
Slr_W90F_r	GATCGCTTGCATAGA**GA**AAACCTCGAAGTTTCTTC

Experimental System

Time-resolved measurements on the Slr1694 mutants presented in this paper, were performed on a visible pump visible probe setup. The system uses a Coherent Legend-USP Ti:S amplifier oscillator (1kHz), providing a light source with a central wavelength of 800nm, bandwidth of 5nm at FWHM, with an average energy of 2.5 mJ/pulse and a duration of ~40 fs. The 800 nm pulses is split in two parts: one part is used to drive an optical parametric amplifier (Coherent OPerA) able to generate light from 468 nm up to 680 nm with an output energy of 2μJ per pulse, which triggers the photo reaction; the remaining fraction of the fundamental 800nm, is focused on a rotating CaF_2 crystal to generate a white-light continuum needed to probe the sample. The polarization between pump and probe beams were set to the magic angle (54.7 °). The probe pulse is focused on the sample by parabolic mirrors to avoid chromatic aberration, for the same reason an achromatic lens (fl:200mm) is used to focus the pump. The pump pulse is progressively delayed respect to the probe using a 60 cm long delay stage (Newport IMS-6000) to cover a time window up to 3.7 ns. The sample, placed in a quartz flow cell of 2 mm optical path, is fixed in the focus plane of the two focusing elements (achromatic lens and parabolic mirror) and circulated by a peristaltic pump. After the sample, the pump, and probe beams are spatially separated; only the

probe beam is collimated in a spectrograph (Oriel) and by this spectrally dispersed across a homebuilt photo-diode array. This 256-pixel array is read out and the data were parsed to a computer calculating the optical densities. Out of the thousand pulses per second, 500 pump-pulses are blocked to allowed to measure the difference in absorption of the white light between molecules pumped and non-pumped.

Data Analysis

The time-resolved data can be described in terms of a parametric model in which some parameters, such as those descriptive of the instrument response function (IRF), are wavelength-dependent, whereas others, such as the lifetime of a certain spectrally-distinct component, underlay the data at all wavelength. The presence of parameters that underlay the data at all wavelength allow the application of global analysis techniques [23], which model wavelength -invariant parameters as a function of all available data. The partitioned variable projection algorithm is well-suited to the optimization of model parameters for global analysis models [30]. The algorithm has the further advantage of estimating the standard error of parameters estimates, an advantage that is useful in model selection and validation. A compartmental model was used to describe the evolution of the spectrally distinct components in time. Global analysis was then applied to estimate the lifetime and relative concentration of each component at each wavelength in the data.

The femtosecond transient absorption data were first globally analyzed using a kinetic model consisting of sequentially interconverting evolution-associated difference spectra (EADS), i.e. 1 → 2 → 3 → ... (Figures 3, 6 and 8, further in the text) in which the arrows indicate successive mono-exponential decays of increasing time constants, which can be regarded as the lifetime of each EADS. The first EADS corresponds to the time-zero difference spectrum. This procedure enables us to clearly estimate the time scales and visualize the evolution of the (excited and intermediate) states of the system.

To disentangle the contributions by the various molecular species in the spectral evolution, we performed a target analysis of time-resolved data. Target analysis involves the application of a compartmental model (i.e., a specific kinetic scheme) containing microscopic decay rates

expressing intercompartmental transitions, and may be used to test detailed hypotheses regarding the underlying kinetics. The spectrum associated with each component in a target analysis applied to difference absorption data is termed species-associated difference spectra (SADS). In contrast to the EADS, the SADS will represent the spectral signature of the pure molecular species and their kinetics after photon absorption. In this way, the reaction mechanism can be assessed in terms of discrete reaction intermediate states.

Results and Discussion

Absorption spectra and photocycle time of Slr1694 mutants

The UV-visible steady-state absorption spectra for dark and light states of the Slr1694 wild type (WT) and mutants are shown in Figure 2. The spectra of WT and W91F are practically identical, with absorption maxima at comparable amplitudes at 442 and 379 nm, assigned to the two lowest excited states S_1 and S_2 of FAD, respectively (Figure 2A). In addition, a vibronic shoulder at 465 nm is resolved. The Y8W mutant shows peaks at 372 and 439 nm with a shoulder at 461 nm and a different ratio between S_1 and S_2 bands. The absorption spectrum of the S28A mutant shows an overall red-shift of the absorption with bands at 387 and 456 nm and a shoulder at 479 nm. Furthermore, the S_2 band is significantly higher than the S_1 band. YcgF from *E. coli*, also called Blrp, contains an alanine at position 28 in its WT form and is equivalent to S28A-Slr1694 mutant [25]. YcgF shows a similar red-shifted steady state absorption with S_2 and S_1 at 382 and 459 nm and a shoulder at 484 nm [9]. The mutation may change the dipolar interaction between this polar residue and the isoalloxazine ring resulting in a red shift of the UV-visible absorption. Alternatively, the FAD wavefunction may slightly extend over the serine, affecting the transition energy [26].

Upon blue-light excitation, WT, the W91F and S28A mutants show a characteristic red-shift of the absorption spectrum (Figure 2B). The Y8W mutant does not show any red-shifted absorption or other long-lived photoproduct. In W91F, the red-shifted spectrum thermally decays to the dark-adapted state in 223 s, which is about 50 times slower than

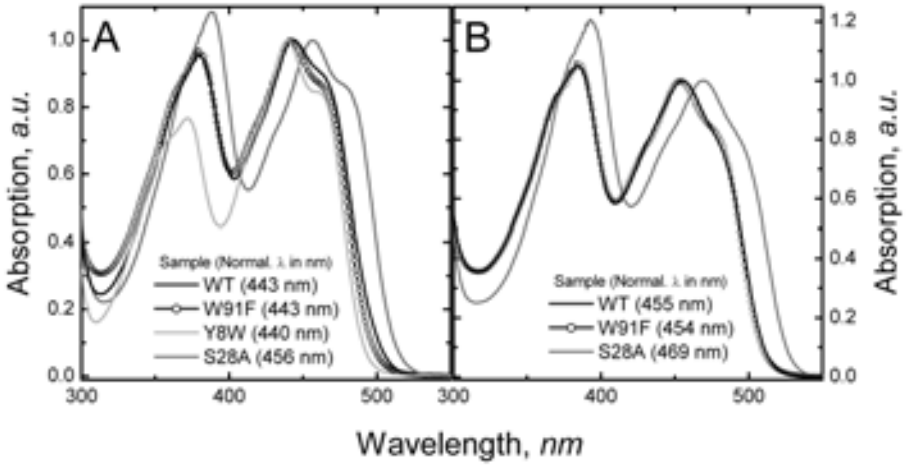

Figure 2. A, steady state absorption in H_2O buffer of the three Slr1694 mutants compared with the Slr1694 wild type. **B**, absorption spectra of the two photocycling mutants in the signaling state compared with that of the Slr1694 wild type. All spectra have been normalized to 1 at the S_1 maximum. The normalization wavelength is reported in brackets for each mutant.

in WT. This is quite remarkable given that in the AppA BLUF domain, the corresponding mutation leads to acceleration of the photocycle [31]. The S28A mutant has a dark recovery of 4 s, essentially the same as in WT.

Ultrafast spectroscopy of Wild type Slr1694

Ultrafast transient absorption spectroscopy on wild type Slr1694 was performed previously in our laboratory [16]. The ultrafast experiments reported in this paper were performed on a different laser setup (see Materials and Methods). For reference and to check reproducibility, we performed experiments on wild type Slr1694, presented in Figure A (EADS) and Figure B (kinetics) of *Appendix*. The results were essentially identical to those of Gauden *et al*, except that in the present experiments the amplitude of the EADS in the FAD ground state bleach region around 450 nm was ca. 30% larger, and that of the induced absorption near 690 nm was 10% larger. These differences probably arise from slightly different spectrospatial overlaps of pump and probe beams and therefore do not affect the interpretation of the spectra. The kinetics were virtually indistinguishable, indicating that the evolution in terms of molecular intermediates was identical between the two experiments.

Ultrafast spectroscopy of the W91F mutant

In the Slr1694 and AppA X-ray structures, the semiconserved residues W91 and W104 have been reported in two conformations, either close to the flavin or in a solvent-exposed position [5, 7]. In its 'W-in' conformation, the indole ring of the tryptophan points towards the flavin at about 4 Å away in Slr1694 (Figure C(A)). In the AppA BLUF domain, the pyrrole nitrogen of W104 hydrogen-bonds to FAD C4=O at a significantly closer distance of 3.3 Å Figure B(B)).

Ultrafast transient absorption spectroscopy was applied to the W91F mutant of the Slr1694 BLUF domain from *Synechocystis* to study its reaction mechanism. The sample was excited at 400 nm and the ensuing absorbance changes were monitored in a spectral window from 420 to 690 nm. The experimental results were globally analyzed in terms of a sequential kinetic scheme with mono-exponentially decaying interconverting species. Figure 3 shows the result of the global analysis procedure in the form of Evolution-Associated Difference Spectra (EADS) for W91F in H_2O (Figure 3A) and in D_2O (Figure 3B). Kinetic traces at selected wavelengths are shown in Figure D of the *Appendix*. Five components were required to fit the data with lifetimes of 1.4 ps (2 ps in D_2O), 16 (16) ps, 90 (138) ps, 380 (590) ps and non-decaying component. The first EADS (Figure 3A, line 1 black) is formed within the instrument response function of ~120 fs and shows a ground state bleach near 450 nm, excited-state absorption around 520 nm, stimulated emission at 550 nm and excited-state absorption at wavelengths longer than ~610 nm. It is associated with singlet excited flavin (FAD^*). Similar spectral signatures for flavin in the lowest singlet excited state have been found for Slr1694 WT [16], Appa WT and mutants [15, 22], flavin in solution [32] and FMN^* in the LOV2 domain of phototropin [33]. The first EADS evolves to the 2nd EADS in 1.4 ps and involves minor spectral changes that include a loss of bleach near 470 nm and a slight blue-shift of the stimulated emission band near 550 nm. This evolution can be assigned to a vibrational cooling process on the excited FAD chromophore [22].

The 2^{nd} EADS has a lifetime of 16 ps and evolves to the third EADS (line 2 gray), which itself has a lifetime of 90 ps. The 3^{rd} EADS shows a decrease of ground state bleaching and stimulated emission, indicating

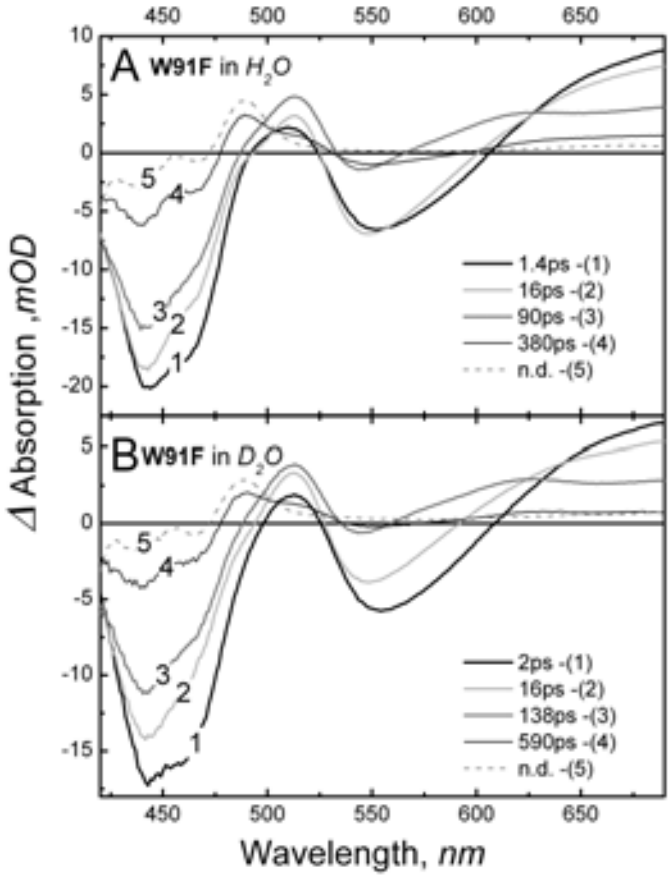

Figure 3: Evolution-associated difference spectra (EADS) resulting from a global analysis on transient absorption experiments on the W91F Slr1694 mutant in: **A**, H_2O buffer; **B**, D_2O buffer. The excitation wavelength was 400 nm.

decay of FAD*, and an increase of absorption near 600 nm. The latter indicates the presence of other molecular species that correspond to FAD radicals, as will be shown below. The fourth EADS (line 4 dark gray) rises in 90 ps and has a lifetime of 380 ps. It shows further decay of ground state bleach and stimulated emission features and a decay of the transient band at 600 nm. A prominent positive band has come up near 490 nm which is indicative of long-lived product ($BLUF_{RED}$) formation [16]. In the last, nondecaying EADS (line 5 dashed), all signs of FAD* or FAD radical species have disappeared and the difference spectrum corresponds to the red-shifted photoactivated state of BLUF domains, $BLUF_{RED}$, apart from a low-amplitude, broad absorption between 550 and 680 nm. The latter may correspond to a small fraction of FAD triplet states, as observed previously in the AppA BLUF domain [15, 22].

The EADS for the W91F mutant in D_2O are shown in Figure 3B. The spectral evolution is similar to that of W91F in H_2O, except that some of the time constants are significantly longer, i.e. 90 ps vs. 138 ps, and 380 ps vs. 590 ps. The overall spectral evolution of the W91F mutant in H_2O and D_2O is quite similar to that of wild type Slr1694 [16].

Target analysis of W91F: assessment of the reaction dynamics

We have shown previously for wild type Slr1694 that the EADS that follow from a sequential global analysis represent a mixture of molecular states [13, 16]. This was primarily related to the multi-exponenential decay of FAD*. To extract the spectral signature of 'pure' molecular species that underlie the molecular transformations, we applied a target analysis [23], using a kinetic scheme that took into account the multiphasic FAD* decay. From the target analysis, species-associated difference spectra (SADS) were derived that corresponded to difference spectra of discrete reaction intermediates. Here, we have applied a similar procedure to the W91F mutant. The kinetic scheme is shown in Figure 4A and consists of 8 compartments: four FAD* compartments that have an identical SADS, two intermediates Q_1 and Q_2, a long-lived product Slr_{RED} and a FAD triplet state (FAD^T). This scheme is identical to that used for wild type Slr1694 [13, 16], except for the triplet compartment. Note that in a target analysis on the AppA BLUF domain, such a triplet state was included [15, 22]. The transient absorption data of W91F in H_2O and D_2O were simultaneously analyzed with a common set of SADS, only allowing for small differences in the FAD^*_{1-4} compartment fractions between H_2O and D_2O. The resulting SADS are shown in Figure 4B, whereas rate constants and fractions of FAD^*_{1-4} contributions are reported in Table 2.

In Figure 4B, the black SADS is associated with FAD*. The target analysis indicates that the decay of FAD^*_{1-4} is highly multiexponential, with time constants of 2.3 ps, 24 ps, 250 ps and 3.3 ns. The time constants were set identical for W91F in H_2O and D_2O, which resulted in slightly different amplitudes for the four compartments (Table 2). The multi-exponentiality most likely is caused by structural flexibility in the FAD binding pocket, particularly of the conserved electron donor Y8 [8, 34]. Such heterogeneity of the ground state was previously observed in

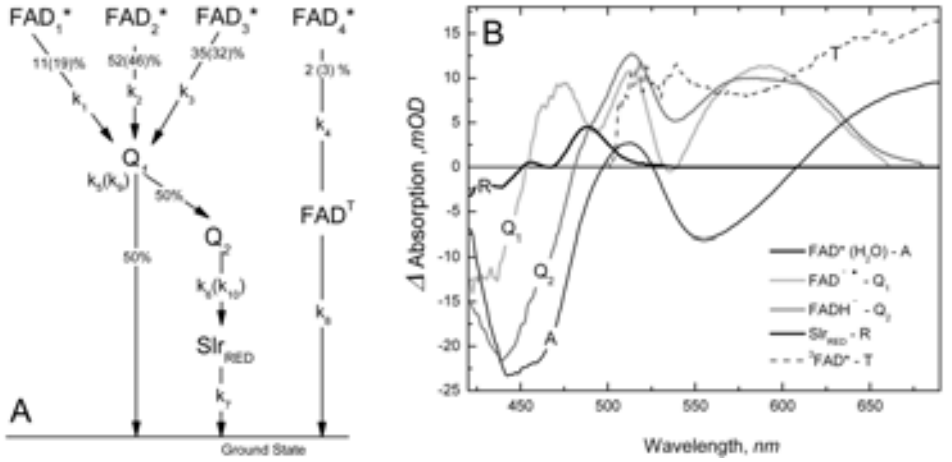

Figure 4: **A**, kinetic model applied in the target analysis for the W91F Slr1694 mutant; **B**, Species-Associated Difference Spectra (SADS) resulting from simultaneous target analysis.

WT-Slr1694 [13, 16] and AppA and its mutants [15, 22, 27]. The absence of an obvious H/D exchange effect on the decay of $FAD*_{1-4}$ indicates that FAD* is deactivated through electron transfer, as for wild type Slr1694 [13, 16].

FAD^*_{1-3} evolve to the first intermediate Q_1. The Q_1 SADS (light gray) shows a positive band at 520 nm and a broad symmetric band near 590 nm. It resembles the absorption difference spectrum of the anionic flavin semiquinone ($FAD^{\bullet-}$) in a charge -transfer (CT) interaction, as previously observed in wild type Slr1694 [16] and in certain flavoenzymes [35]. As in the wild type, Q_1 is associated with a molecular species $FAD^{\bullet-}$ + $Y8^{\bullet+}$ [13, 16]. Q_1 is short-lived and its SADS is therefore hard to estimate. It decays in 5 ps (11 ps in D_2O), forming the second intermediate Q_2 at a yield of 50%. About half of the $FAD^{\bullet-}$ + $Y8^{\bullet+}$ radical pairs decay to the ground state through charge recombination [16]. The Q_2 SADS (dark gray) has a broad absorption between 480-680 nm with maxima at 575 and 605 nm. This SADS is assigned to a neutral semiquinone flavin radical $FADH^{\bullet}$ [16, 36] that is formed upon proton transfer from Y8 [13]. Q_2 represent a neutral radical pair $FADH^{\bullet}$ + $Y8^{\bullet}$. Radical-pair recombination with ensuing decay of $FADH^{\bullet}$ occurs in 75 ps (130 ps in D_2O), forming the non-decaying Slr_{RED} species (bold black), with its typical absorption peak at 489 nm, which is characteristic of the BLUF signaling state.

Table 2: Rate constants and branching parameter for W91F Slr1694 mutant

	FAD_1*	FAD_2*	FAD_3*	FAD_4*	Q_1	Q_2	Slr_{RED}	FAD^T
FAD_1*								
FAD_2*								
FAD_3*								
FAD_4*								
Q_1	k_1, 11(19)%	k_2, 52(46)%	k_3, 35(32)%		k_5, (k_9)			
Q_2					k_5, (k_9)			
Slr_{RED}						k_6, (k_{10})	k_7	
FAD^T				k_4, 2(3)%				k_8

k_1 = 442E-03	$\tau_1=(k_1)^{-1}$=2.26 ps
k_2 = 425E-04	$\tau_2=(k_2)^{-1}$=23.5 ps
k_3 = 402E-05	$\tau_3=(k_3)^{-1}$=250 ps
k_4 = 300E-06	$\tau_4=(k_4)^{-1}$= 3.3 ns
k_5 = 206E-03	$^{H2O}\tau_{Q1}=(k_5)^{-1}$= 4.8 ps
k_6 = 134E-4	$^{D2O}\tau_{Q1}=(k_9)^{-1}$=11 ps
$k_7 \rightarrow$0.0	$^{H2O}\tau_{Q2}=(k_6)^{-1}$=75 ps
$k_8 \rightarrow$ 0.0	$^{D2O}\tau_{Q21}=(k_{10})^{-1}$=130 ps
k_9 = 934E-4	$\tau_{SlrRED}=(k_7)^{-1} \rightarrow$ n.d.
k_{10} = 786E-5	$\tau_{FADT}=(k_8)^{-1} \rightarrow$ n.d.

As observed previously for wild type Slr1694, a minor fraction of excited FAD (FAD^*_4) does not feed into the productive photocycle. The target analysis results in a lifetime of 3.3 ns for FAD^*_4. Given such a timescale, it is expected that a major part of this FAD* fraction undergoes intersystem crossing to the FAD triplet state (FAD^T,dashed T line in Figure 4B [33]). Reliable spectral estimation of FAD^T is only possible in the part of the spectrum where its SADS is sensibly different from the other SADS. To estimate the FAD^T SADS, the ground state bleach part from 420 to 500 nm was set identical to that of the singlet excited state FAD* and a low weight was assigned to the FAD^T SADS between 420 and 500 nm assigned in the fitting procedure to avoid compensation effects with flavin ground state bleach present in the SADS of FAD^*_{1-4}, Q_1, Q_2 and Slr_{RED}. The resulting FAD^T SADS shows a broad, positive absorption from 500 to 690 nm, with a spectral shape that is similar to that observed

in the AppA BLUF domain [22] and the LOV_1 and LOV_2 domains of phototropin [33, 37, 38].

Slr_{RED} quantum yield in W91F

For AppA, it was shown previously that the quantum yield of $BLUF_{RED}$ formation is ~40% higher in the W104F mutant (0.37) as compared to wild type (0.24) [15, 31]. This was explained by a competing non-productive electron transfer pathway from W104 to FAD in wild type AppA. Upon removal of W104, this electron transfer pathway was eliminated, leading to a longer excited-state lifetime and increased $BLUF_{RED}$ quantum yield. To examine whether such a phenomenon occurs in Slr1694 as well, Figure 5 shows a comparison of the signal amplitudes of FAD^* and Slr_{RED} for wild type Slr1694 and the W91F mutant. The amplitudes of FAD^* ground state bleach at early times at 450 nm and the $BLUF_{RED}$ absorption at 489 nm are similar for wild type Slr1694 and the W91F mutant. This observation shows that the quantum yields for $BLUF_{RED}$ formation in wild type and W91F mutant are not significantly different, and amount to ca. 0.40 [16]. Also, the FAD^* lifetimes in wild type and W91F are quite similar. The two intermediates that lead to the red form, identified as Q_1-$FAD^{\bullet-}$-$Y8^{\bullet+}$, and Q_2 - $FADH^{\bullet}$-$Y8^{\bullet}$, are formed and decay with essentially identical lifetimes compared to the WT (see Table 3). The similarities in the photocycle and quantum yield for the signaling state formation demonstrate that W91 is not required for Slr1694 photoactivation nor does it provide a significant pathway for electron transfer to FAD that competes with productive electron transfer from Y8.

Ultrafast spectroscopy of the S28A mutant

From structural data on Slr1694 the semi-conserved S28 is observed in two conformations of the side chain with one close to heterocyclic ring of the flavin chromophore, as shown in Figure E, and another coordinating the backbone (not shown). The near distances of the serine oxygen atom to the heteroatoms of the flavin range from 4.8 Å (C_2O) to 3.5 Å (N_5). The proximity of S28 to FAD suggests that S28 may act as a proton donor to FAD at some point in the photochemical reaction cycle.

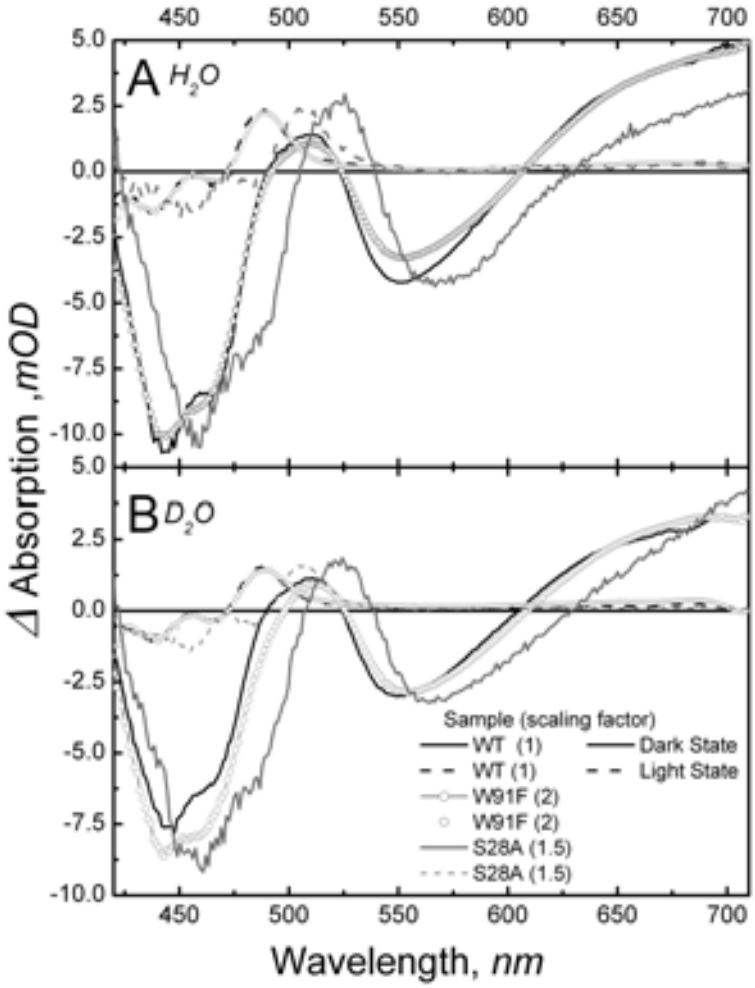

Figure 5: Estimation of the signaling state quantum yield of the two photocycling mutants in H_2O (**A**) and D_2O (**B**). The continuous-line SADS, associated to the excited flavin (FAD^*), have been scaled to have equal ground state bleach near 450 nm. Such scaling numbers, reported in brackets, have been used to rescale the dashed-lines SADS, associated to the long-lived signaling state.

Table 3 Time constants associated with the SADS for Slr1694 wild type compared with W91F, Y8W and S28W Slr1694 mutants. Time in ps.

	WT	W91F	Y8W	S28A
^{hot}**FAD***	n.r.	n.r.	n.r.	0.5
FAD$_1$*	6 (7)	2	1 (0.77)	5
FAD$_2$*	26 (28)	24	8	20
FAD$_3$*	92 (94)	250	n.r.	115
FAD$_4$*	335 (354)	3300	n.r.	n.r.
Q$_1$	6 (20)	5 (11)	10 (18)	37 (110)
Q$_2$	67 (160)	75 (130)	206 (332)	n.r.
Q$_3$	n.r.	n.r.	4300	n.r.
Slr$_{RED}$	6s (20s)	223s	n. ph.	5s
FAD^T	n.r.	n.r.	n.r.	nr.

n.r.: not recorded; **n.ph**.; not photocycling

Femtosecond transient absorption experiments were performed on the S28A mutant of the Slr1694 BLUF domain. The EADS that result from a sequential analysis of the time-resolved data are presented in Figure 6 (A-H_2O, B-D_2O), with kinetic traces at selected wavelengths shown in Figure F of *Appendix*. Six kinetic components were required to fit the data in H_2O (D_2O), with lifetimes of 0.5 ps (black EADS), 2 (2.7) ps (light gray, 2-EADS), 10 (16) ps (gray, 3-EADS), 96 (90) ps (dark gray, 4), 325 (610) ps (light gray dashed, 5) and a non-decaying component (dark gray dashed, 6-EADS). The subpicosecond component could be resolved in this particular dataset because of a cross-phase modulation artifact weaker than in the other mutants. However, due to the instability of the long-lived photoproduct of the S28A mutant, the overall S/N ratio of this particular dataset is lower than those obtained on wild type Slr1694 and other mutants. The 0.5 ps EADS represents a mixture of the initially excited S_2 and S_1 excited states of FAD [22]. After internal conversion in 0.5 ps, the 2 (2.7) ps EADS represents the lowest singlet excited state of FAD, denoted as FAD*. The third and fourth EADS with lifetimes of

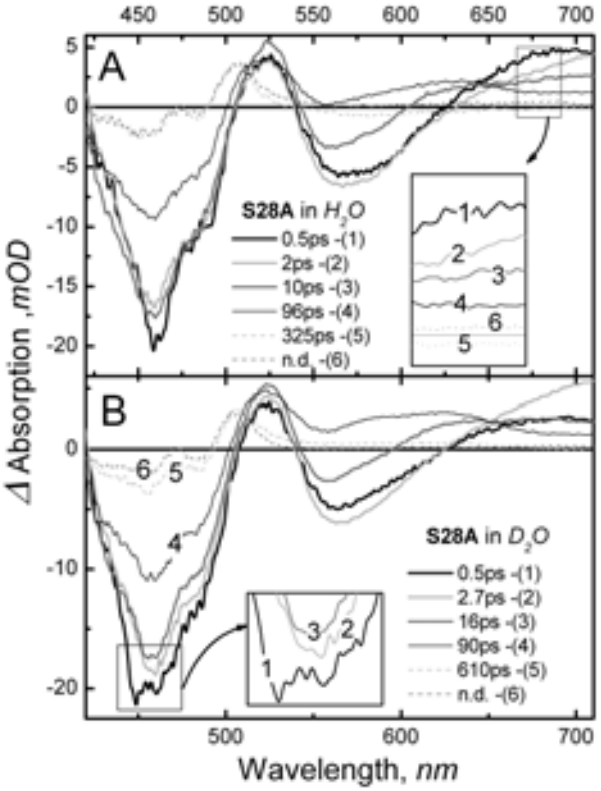

Figure 6: EADS resulting from global analysis for the S28A Slr1694 mutant in: **A**, H2O buffer; **B**, D2O buffer.

10 ps and 96 ps are a mixture of FAD* and flavin radical species absorbing in the central part of the spectrum at above 550 nm. The fifth, 325 ps EADS corresponds to mainly the long-lived $BLUF_{RED}$ photoproduct. The small-amplitude negative-going signal at ~580 nm is hardly resolved given the poor signal-to-noise ratio in this particular experiment. If significant at all, it may correspond to a small fraction of unbound FAD*. The sixth, nondecaying EADS represents the photoproduct $BLUF_{RED}$, which absorbs near 505 nm in this particular mutant. As for the W91F mutant, the overall spectral evolution of this mutant is similar to that of WT-Slr1694 [16].

Target analysis of S28A: assessment of the reaction dynamics

For a more complete, quantitative understanding of the photochemistry of the S28A mutant, a target analysis has been applied to the time-resolved data. The kinetic scheme employed and the SADS resulting from the

target analysis are displayed in Figure 7. The kinetic scheme is similar to that of wild type and W91F, except that only one intermediate (Q_1) is used to connect FAD^* to Slr_{RED}. The lifetimes of each compartment are reported in Table 3; rate constants and fractional contributions are reported in Table 4. The FAD_{S1-S2} ($^{hot}FAD^*$, "h" thin black line in Figure 7B) compartment decays on a subpicosecond timescale (0.5 ps) to populate FAD^*_{1-3}. These three singlet excited states of flavin have identical SADS (the bold blak line, F-SADS Figure 7B) but different decay times. $FAD^*_{1,2}$ relaxation occurs in 5 and 20 ps, mainly (~80%) through Q_1 and a minor fraction (~20%) directly to the ground state. FAD^*_3 decays entirely to the ground state with a lifetime of 115 ps. The short FAD^* lifetimes are similar to those of WT, as FAD^*_{1-2} decay in 5 and 20 ps and 6 and 26 ps in S28A and WT, respectively. The nonproductive component FAD^*_3 has a lifetime of 115 ps in S28A, which is twice as short as in WT (335 ps; see comparison in Table 3). As for wild type and W91F, the decay of FAD^*_{1-3} does not show any effect of H/D exchange, indicating that FAD^* is deactivated through electron transfer [13, 16]. Q_1 is populated from FAD^*_{1-2}. Its SADS (light gray line), resembles the spectrum of the FAD neutral semiquinone ($FADH^\bullet$) that was previously identified in the wild type Slr1694 [16] and the W91F mutant described above. $FADH^\bullet$ evolves to the Slr_{RED} compartment (dark gray, R-line) with a time constant of 37 ps in H_2O and 110 ps in D_2O.

In the target analysis of the WT and W91F mutant, two intermediates en route to the Slr_{RED} product were identified, $FAD^{\bullet-}$ and $FADH^\bullet$. For the S28A mutant, only one intermediate, $FADH^\bullet$, could be extracted from the time-resolved data. By its nature, the $FAD^{\bullet-}$ intermediate is short-lived (5 – 20 ps in WT and W91F, in H_2O and D_2O respectively) and difficult to detect. Given the relatively low signal to noise ratio in the S28A experiments, the $FAD^{\bullet-}$ intermediate may have escaped detection.

The S28A mutant shows a significant red shift in the UV-visible absorption spectrum, both in the dark and after illumination (Figure 2A and B). This may be due to disruption of a specific interaction (H-bond or dipolar interaction) between FAD and serine compared with the native S28 [26]. Despite this obvious effect from the serine on the steady-state absorption properties, the photochemistry of the S28A mutant is very similar to that of wild type. Notably, however, the evolution from Q_2 to the Slr_{RED} product state is about two times faster in S28A as compared

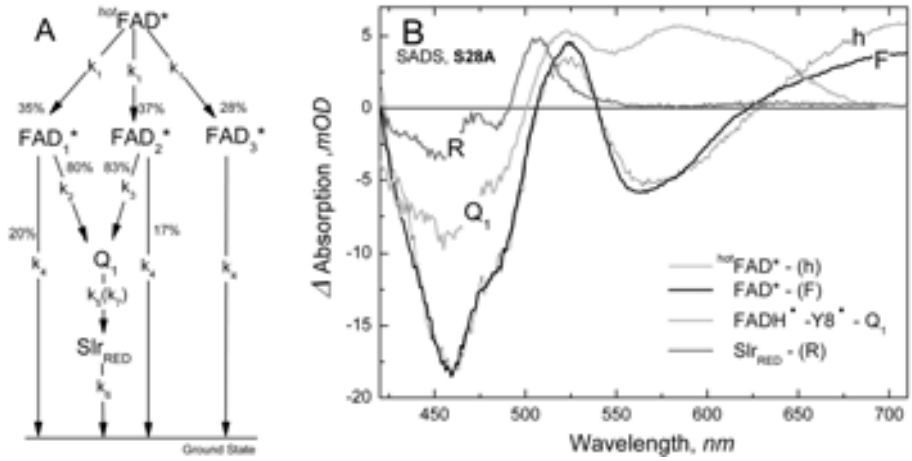

Figure 7: **A**, kinetic model applied in the target analysis for the S28A Slr1694 mutant; **B**, SADS resulting from simultaneous target analysis.

to WT and the W91F mutant (see Table 3). Like W91F, the S28A mutant does not exhibit a change of quantum yield of signaling state formation (Figure 5, gray unbroken and dashed lines). In addition, the lifetime of the FAD singlet excited and the dark-state recovery of the red-shifted product state are not affected significantly (Table 3). We conclude that S28 is not required or significantly involved in the initial light-driven

Table 4 Rate constant and fraction decay estimated for S28A mutant using target analysis.

	^{hot}FAD*	FAD$_1$*	FAD$_2$*	FAD$_3$*	Q$_1$	Slr$_{RED}$
^{hot}FAD*						
FAD$_1$*	k_1, 35%	k_4, 20%				
FAD$_2$*	k_1, 37%		k_4, 17%			
FAD$_3$*	k_1, 28%			k_4		
Q$_1$		k_2, 80%	k_3, 83%			
Slr$_{RED}$					k_5,(k_7)	k_6

k_1 = 217E-02	$\tau_{hot}=(k_1)^{-1}$=0.46 ps
k_2 = 216E-03	$\tau_1=(k_2 + k_4)^{-1}$=4.5 ps
k_3 = 430E-04	$\tau_2=(k_3 + k_4)^{-1}$=20 ps
k_4 = 870E-05	$\tau_3=(k_4)^{-1}$= 115 ps
k_5 = 268E-04	$^{H2O}\tau_{Q1}=(k_5)^{-1}$= 37 ps
$k_6 \rightarrow$ 0.0	$^{D2O}\tau_{Q1}=(k_7)^{-1}$=110 ps
k_7 = 907E-05	$\tau_{SlrRED}=(k_6)^{-1} \rightarrow$ n.d.

hydrogen-bond switch reaction, and does not, for instance, act as a proton donor to FAD after its initial reduction to $FAD^{\bullet -}$ by tyrosine. Possibly, S28 has a role in signal transmission to the molecular surface at a later stage of the photoreaction [26].

Ultrafast spectroscopy of the Y8W mutant

Since no crystal structure of the Y8W mutant is available, we introduced a tryptophan residue replacing Y8 by homology modeling. The structural model of the Y8W mutant of Slr1694 was refined using the Swiss-Model homology-modeling server [39]. As a template the pdb-file 2hfnA was used [7]. The indole side chain is situated in the aromatic plane of the tyrosine residue but the aromatic system is extended towards the xylene moiety of the isoalloxazine resulting in 0.5 Å shorter distance. However, if the oxygen atom of the tyrosine is considered, the distances for a dipolar or proton exchange interaction are still shorter in the wild-type protein. Especially the distance of the tyrosine oxygen to N5 is smaller than from the indole nitrogen. Note that W8 is unlikely to hydrogen bond with Q50, which makes it difficult to assess the conformation of the latter side chain.

The photochemistry of the Y8W mutant was investigated by femtosecond time-resolved absorption spectroscopy after 400 nm laser pulse excitation. The EADS resulting from global analysis are shown in Figure 8. Four components were required to adequately describe the time resolved data, with lifetimes of 1 ps, 11 (18) ps, 76 (100) ps in H_2O (D_2O) plus one non-decaying component. The black EADS in Figure 8 (A-H_2O; B-D_2O), is similar to the initial EADS in wild type and the W91F and S28A mutants, and assigned to FAD*. This EADS decays in 1 ps to form the 2nd EADS, which has a lifetime of 18 ps (light gray line). The 2nd EADS shows a slightly reduced ground state bleach at 450 nm and a broad induced absorption at wavelengths longer than 475 nm, with a double-peak like structure around 600 nm. In addition, a dip near 550 nm may be due to a remaining fraction of stimulated emission. We ascribe the 2nd EADS to a mixture of a FAD radical and FAD* (see below). The 2nd EADS spectrum evolves into the 3rd EADS (dark gray line) in 11 ps (18 ps in D_2O). This EADS is characterized by a sharp drop in the FAD ground state bleach and induced absorption at longer wavelengths. With maxima at 550 and

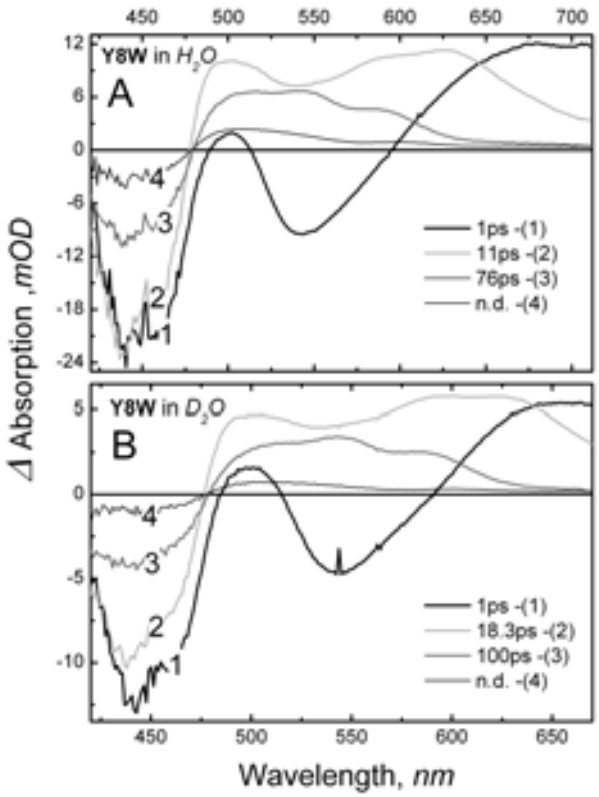

Figure 8: EADS resulting from global analysis for the Y8W Slr1694 mutant in: **A**, H_2O buffer; **B**, D_2O buffer.

~580 nm, the spectral shape of the induced absorption does not carry any spectral features associated with FAD* or the previous EADS. The 3rd EADS evolves in 76 ps (100 ps in D_2O) into the long-lived EADS (thin black line) which does not decay on the timescale of our experiment. It is characterized by further reduction of the overall signal amplitude. It possesses an induced absorption near 520 nm that tails off to the red.

Target analysis of Y8W: identification of three different radical pairs

Upon replacement of Y8 with W, the long-lived signaling state is not formed, but photoinduced electron and proton transfer to FAD still occurs. To better understand the photochemical events in the Y8W mutant, the time-resolved data was subjected to a target analysis using the kinetic scheme displayed in Figure 9A. The scheme was chosen because it employs the minimum number of compartments (four),

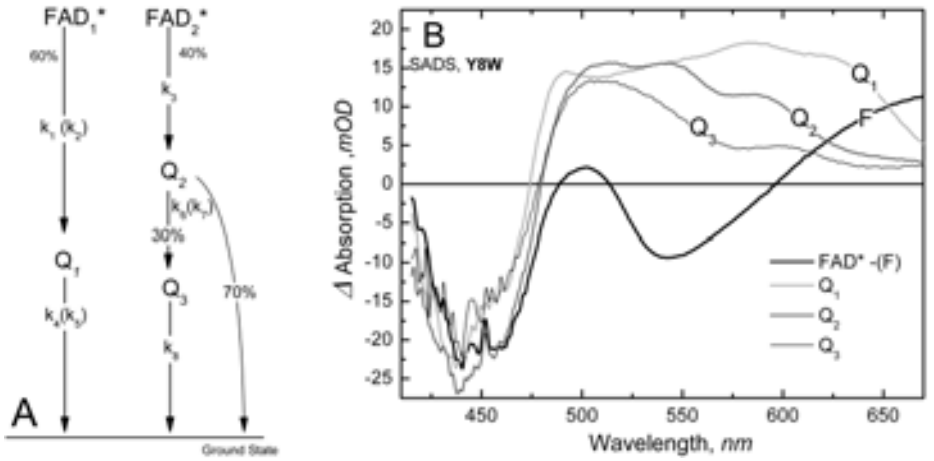

Figure 8: EADS resulting from global analysis for the Y8W Slr1694 mutant in: **A**, H_2O buffer; **B**, D_2O buffer.

provides the lowest root mean square error (RMS) and allowed a physically reasonable interpretation. In the analysis, we identified four different molecular species, $FAD^*_{1,2}$, Q_1, Q_2 and Q_3. Note that because the Y8W photochemistry is so much different from that of wild type, Q_1 and Q_2 do not necessarily bear a direct relationship to Q_1 and Q_2 identified in wild type Slr1694 BLUF [13, 16]. The SADS that result from the target analysis are reported in Figure 9B.

The $FAD^*_{1,2}$ SADS (black line-F) is essentially identical to those resolved for the W91F and S28A mutants (Figure 4B and Figure 7B, respectively). FAD^*_1 evolves to Q_1 (light gray SADS) in about 1 ps. Q_1 is characterized by a broad positive absorption spanning from 475 to 685 nm with peaks at 480, 585 and 625 nm. It resembles the absorption of a neutral semiquinone flavin radical, $FADH^\bullet$ that is red-shifted in comparison to $FADH^\bullet$ in wild type Slr1694. Q_1 recombines to the ground state showing a strong H/D exchange effect (10 and 18 ps in H_2O and D_2O). The latter observation indicates that radical-pair recombination, probably involving hydrogen back-shuttling from FAD to the electron/proton donor, occurs.

Interestingly, the decay of FAD^*_1 is slightly faster in D_2O (0.77 ps) as compared to H_2O (1.1 ps). This phenomenon can be observed in the kinetics (Figure G, *Appendix*), where the decay of stimulated emission (545 nm) and the rise of the radical intermediate (605 nm) is slightly faster in the Y8W mutant in D_2O as compared to H_2O. Such an inverted

KIE is unexpected because in BLUF domains, electron transfer usually is considered to constitute the primary photochemical reaction [13-16, 40]. In addition, if proton or hydrogen transfer underlies FAD^*_1 in Figure 9A deactivation, one would under most circumstances expect a slowdown of the reaction upon H/D exchange. Inverted KIE's have been reported in the literature [41, 42]. If in Y8W the decay of FAD^*_1 indeed corresponds to electron transfer, its fast rate of ~ $(1\ ps)^{-1}$ could be mediated by specific collective nuclear motions, as for instance shown for the photosynthetic reaction center [43, 44]. A downshift of such nuclear motions upon H/D exchange may result in an increased coupling with the charge separated state, effectively speeding up the electron transfer rate. Obviously, the inverted KIE phenomenon in the Y8W mutant requires further investigation.

FAD^*_2, which represents 40% of the excited-state decay, evolves via rate constant k_3 to form Q_2 (bold dark gray SADS). 30% of Q_2 , formed with a rate constant of $(8\ ps)^{-1}$ decays with a rate constant k_6 (k_7 in D_2O) to form Q_3 (green SADS), and whereas 70% recombines to the ground state (Table 3, kinetic scheme in Figure 9A and Table 5). The Q_2 SADS shows a ground state bleach around 450 nm and a positive absorption for wavelengths longer than 480 nm, with three peaks at 510, 547 and 585 nm. As for Q_1, the ground state bleach indicates that Q_2 is associated with a flavin species. The absorption maxima at 547 and 585 nm resemble the $FADH^\bullet$ spectrum identified in wild type Slr1694 [16]. The observation of an absorption at 500 nm that is equally high, or higher than the maximum at 547 and 585 nm indicates that other molecular species may be involved in this SADS. The absorption near 500 nm probably corresponds to a neutral tryptophanyl radical $W^\bullet$ [45], so that Q_2 corresponds to $FADH^\bullet - W^\bullet$.

The Q_3 SADS (thin dark gray SADS) features the flavin ground state bleach near 450 nm and an induced absorption above 480 nm. It is formed from Q_2 with a yield of 30% and recombines to the ground state in 4.3 ns. The Q_3 species is spectroscopically very similar to a species called 'R' in the AppA Y21I mutant [15]. The latter species was tentatively assigned to a $FAD^{\bullet-}$ radical, possibly in combination with a $W^\bullet$ tryptophanyl neutral radical, ($FAD^{\bullet-} - W^\bullet$) which both absorb around 520 nm [35, 45]. Alternatively, the low absorption near 600 nm may be due to a $W^{\bullet+}$ radical cation [45], consistent with a $FAD^{\bullet-} - W^{\bullet+}$ radical pair.

Table 5 Rate constant and fraction decay estimated for Y8W mutant using target analysis.

	FAD_1*	FAD_2*	Q_1	Q_2	Q_3
FAD_1*					
FAD_2*					
Q_1	k_1 (k_2), 60%		k_4 (k_5)		
Q_2		k_3, 40%		k_6 (k_7), 70%	
Q_3				k_6 (k_7), 30%	k_8

k_1 = 885E-03	$\tau_1=(k_1)^{-1}$= 1.1 ps
k_2 = 1298E-03	$\tau_2=(k_2)^{-1}$= 0.77 ps
k_3 = 1241E-04	$\tau_3=(k_3)^{-1}$=8.0 ps
k_4 = 1035E-04	$^{H2O}\tau_{Q1}=(k_4)^{-1}$= 9.7 ps
k_5 = 565E-04	$^{D2O}\tau_{Q1}=(k_5)^{-1}$= 17.7 ps
k_6 = 485E-05	$^{H2O}\tau_{Q2}=(k_6)^{-1}$= 206 ps
k_7 = 301E-05	$^{D2O}\tau_{Q2}=(k_7)^{-1}$= 332 ps
k_8 = 2315E-07	$\tau_{Q3}=(k_8)^{-1}$= 4.3 ns

The target analysis on Y8W indicates that as in most BLUF domain dynamics, FAD* has a multi-exponential decay [13-16, 22, 31, 40] This was assigned to conformational flexibility of the FAD binding pocket [27, 34], resulting in a heterogeneity of distances between FAD and the primary electron donor, Y8 [15]. In the Y8W mutant, the W being more bulky than Y, may be restricted in its movement but may nevertheless find two different orientations respect to FAD. The fact that FAD^*_1 and FAD^*_2 have almost the same starting population upon the photoexcitation (60 and 40%, respectively; see Table 5 and kinetic scheme in Figure 9A), indicate that the two orientations are almost isoenergetic.

In contrast to other BLUF domains, the different FAD* decay phases of the Y8W mutant feed into distinct reaction pathways, leading to different transient intermediates. In Y8W, two separate deactivation pathways for the excited flavin are observed. The FAD^*_1 deactivation pathway is fast (~ 1 ps) and involves ~60% of the initially excited flavin population, which results in transient $FADH^\bullet$ neutral radical formation. The second deactivation pathway for the photo-excited flavin is slower and involves the remaining ~40% of the initially excited FAD that decays in 8 ps. FAD^*_2 evolves to neutral flavin semiquinone Q_2 ($FADH^\bullet$) in 8 ps, which, in turn, evolves in an anionic semiquinone Q_3 ($FAD^{\bullet-}$) in 206 ps

(332 ps in D_2O, see Table 1 and Table 5). Notably, Q_1 and Q_2 both correspond to $FADH^{\bullet}$, but the former is 40 nm red-shifted with respect to the latter, which indicates different interactions with the protein matrix, possibly via alternative hydrogen-bond patterns.

Electron and proton transfer to FAD in BLUF domains occurs through nearby aromatic side chains, as demonstrated for the AppA BLUF domain where deletion of Y21 and W104 has lead to complete abolishment of electron transfer [15]. The only candidates are the introduced W8 and the native W91 For Q_1 and Q_2, the redox partner of the protonated flavin is ascribed to $W^{\bullet}$, which has its spectroscopic signature in the positive band near 510 nm. For the de-protonated flavin anion semiquinone radical Q_3, the partner could be either $W^{\bullet}$ or tryptophan radical cation ($W^{\bullet+}$) which have their absorption between 480 and 670 nm [34, 46, 47]. The question arises whether Y8 or W91 acts as redox partners to FAD in the Y8W photochemistry. In the homology modeling, W8 is located at 4.6 Å from FAD (Figure H), whereas W91 is located at a distance of 4 Å in the 'W-in' conformation (Figure C(B)). Given these similar distances and the favorable midpoint potential of W [48], W8 as well as W91 may act as electron donor to FAD.

In WT, W91 does not or hardly participate in electron transfer to FAD (see the comparison between wild type and W91F above). However, in the Y21I mutant of the AppA BLUF domain, which only contains the homologous W104 as potential redox partner to FAD, it was observed that electron transfer from W104 to FAD was significantly faster than in wild type AppA (~15 ps vs hundreds of ps, respectively) [15]. This increase of electron transfer rate was assigned to a change of midpoint potential that may have resulted from altered H-bonding patterns in the FAD binding pocket, or slightly altered donor-acceptor distances. In fact, the FAD^*_2 electron/proton transfer pathway involving Q_2 ($FADH^{\bullet}$) and Q_3 ($FAD^{\bullet-}$) is spectrally and temporally remarkably similar to that observed in Y21I mutant of AppA (the 'Q' and 'R' intermediates in ref. [15]), which suggests that W91 is the redox partner of FAD in this deactivation branch. In such a case, W91 will take the 'in' position in close vicinity to FAD [6, 7]. Involvement of W8 cannot, however, be excluded.

In the FAD^*_1 deactivation pathway, the redox partner of FAD in the radical pair formation may either correspond to W8 or W91. If W8 is the redox partner, rapid electron and proton transfer from W8 to FAD occurs in 1 ps, followed by radical-pair recombination in 10 ps (18 ps in D_2O). In

this scenario, the FAD^*_1 and FAD^*_2 deactivation branches represent two significantly different conformations of the FAD binding pocket, because the fast electron transfer from W8 to FAD in 1 ps in the 'FAD*1 conformation' is essentially shut down in the 'FAD*2 conformation'. This will only occur if W8 in the 'FAD*2 conformation' has an increased distance to FAD to the extent that its electron transfer rate slows down more than an order of magnitude as compared to the FAD*1 conformation. If, on the other hand, W91 would be the electron donor in the FAD*1 deactivation pathway, it would imply that (i) electron transfer from W8 cannot compete with that from W91 and (ii) a different $FADH^\bullet$ – $W91^\bullet$ radical pair is formed with respect to the FAD*2 deactivation pathway, with a red-shifted $FADH^\bullet$ absorption (Figure 9B). This could be explained by different H-bonding to FAD in the FAD^*_1 and FAD^*_2 conformations. It should be noted, however, that H-bonding to FAD is expected to affect the energy of electronic transitions [49, 50], and therefore the absorption spectrum of the Y8W mutant should have a fine structure of its vibronic progression at 444 and 470 nm, as for instance recently demonstrated for the LOV2 domain of phototropin [51]. Such heterogeneity in absorption maxima is not observed in the steady-state absorption spectrum of the Y8W mutant (Figure 2) nor in its second derivative (not shown). Therefore we tentatively assign W8 as the redox partner to FAD in the FAD^*_1 decay branch.

Conclusions

We have utilized ultrafast spectroscopy to characterize the photochemistry of Slr1694 mutants in which the putative electron and proton donors S28, W91 and Y8 have been removed and replaced by side chains with altered reactivity. The key residue for primary electron transfer, Y8, was substituted by tryptophan to verify if this side chain can transfer electrons and protons to FAD and possibly stabilize reaction intermediates for further studies. The conformational heterogeneity in the Y8W mutant results in two distinct deactivation pathways for the excited flavin. These pathways, characterized by different dynamics, are interpreted as distinct protein populations with two different, nearly iso-energetic conformations of the introduced tryptophan. The introduced W is likely to act as electron and proton donor to FAD to result

in a short-lived radical pair that recombines on the picosecond timescale. The introduced W lacks the ability to stabilize the BLUF signaling state or any long-lived chemical species.

Removal of the hydroxyl group of the semi-conserved side chain S28 resulted in photoactivation dynamics that revealed only one reaction intermediate, assigned to a FAD neutral semiquinone. Because the decay of the excited flavin is not sensitive to H/D exchange, electron transfer from Y8 to FAD is considered to be the rate-limiting event as in wild type Slr1694. The quantum yield of signaling state formation and dark state recovery remains comparable with what found for the wild type. Overall, our findings indicate that S28 does not play a vital role for the photoactivation of the Slr1694 protein. The BLUF domain of YcgF from *E. coli* does not contain serine a this position and is strikingly similar to the S28A mutant with respect its red shifted absorption of both dark and signaling state [9, 25].

The transient absorption measurement on W91F mutant finally showed, that in Slr1694 W91 hardly participates in the photoactivation process, since photochemistry and quantum yield of the signaling state remain unchanged by this mutation. Besides, a longer living flavin excited state results in a formation of a small amount of flavin triplet. The dark recovery time is significantly increased. The results from ultrafast studies on mutated BLUF domains enabled us to rule out a general role in the initial photochemistry of two semi-conserved amino acids S28 and W91 for other so far investigated related BLUF proteins.

Acknowledgments

The authors thank Maxime T.A. Alexandre for stimulating discussions, Gabriele Reinke for excellent technical assistance and Cathrin Lempfuhl for protein preparation. This work was supported by the European Union through the LaserLab Europe Access Programme (T.M. and P.H.). C.B. was supported by the Life Sciences Councel of the Netherlands Organization for Scientific Research (NWO-ALW). K.M.M by was supported by Computational Science grant #635.000.014 from NWO. J.T.M.K. was supported by NWO-ALW through a VIDI fellowship.

References

1. Gomelsky M, Klug G: **BLUF: a novel FAD-binding domain involved in sensory transduction in microorganisms**. *Trends Biochem Sci* 2002, **27**(10):497-500.
2. Iseki M, Matsunaga S, Murakami A, Ohno K, Shiga K, Yoshida K, Sugai M, Takahashi T, Hori T, Watanabe M: **A blue-light-activated adenylyl cyclase mediates photoavoidance in Euglena gracilis**. *Nature* 2002, **415**(6875):1047-1051.
3. Masuda S, Bauer CE: **AppA is a blue light photoreceptor that antirepresses photosynthesis gene expression in Rhodobacter sphaeroides**. *Cell* 2002, **110**(5):613-623.
4. Anderson S, Dragnea V, Masuda S, Ybe J, Moffat K, E.Bauer C: **Structure of a novel photoreceptor, the BLUF domain of AppA from Rhodobacter sphaeroides**. *Biochemistry* 2005, **44**(22):7998-8005.
5. Jung A, Domratcheva T, Tarutina M, Wu Q, Ko WH, Shoeman RL, Gomelsky M, Gardner KH, Schlichting I: **Structure of a bacterial BLUF photoreceptor: Insights into blue light-mediated signal transduction**. *P Natl Acad Sci USA* 2005, **102**(35):12350-12355.
6. Jung A, Reinstein J, Domratcheva T, Shoeman RL, Schlichting I: **Crystal structures of the AppA BLUF domain photoreceptor provide insights into blue light-mediated signal transduction**. *J Mol Biol* 2006, **362**(4):717-732.
7. Yuan H, Anderson S, Masuda S, Dragnea V, Moffat K, Bauer CE: **Crystal structures of the Synechocystis photoreceptor Slr1694 reveal distinct structural states related to signaling**. *Biochemistry* 2006, **45**(42):12687-12694.
8. Grinstead JS, Avila-Perez M, Hellingwerf KJ, Boelens R, Kaptein R: **Light-induced flipping of a conserved glutamine sidechain and its orientation in the AppA BLUF domain**. *Journal of the American Chemical Society* 2006, **128**(47):15066-15067.
9. Hasegawa K, Masuda S, Ono TA: **Light induced structural changes of a full-length protein and its BLUF domain in YcgF(Blrp), a blue-light sensing protein that uses FAD (BLUF)**. *Biochemistry* 2006, **45**(11):3785-3793.
10. Masuda S, Hasegawa K, Ishii A, Ono TA: **Light-induced structural changes in a putative blue-light receptor with a novel FAD binding fold sensor of blue-light using FAD (BLUF); Slr1694 of Synechocystis sp PCC6803**. *Biochemistry* 2004, **43**(18):5304-5313.
11. Unno M, Masuda S, Ono TA, Yamauchi S: **Orientation of a key glutamine residue in the BLUF domain from AppA revealed by mutagenesis, spectroscopy, and quantum chemical calculations**.

Journal of the American Chemical Society 2006, **128**(17):5638-5639.

12. Unno M, Sano R, Masuda S, Ono TA, Yamauchi S: **Light-induced structural changes in the active site of the BLUF domain in AppA by Raman spectroscopy**. *Journal of Physical Chemistry B* 2005, **109**(25):12620-12626.
13. Bonetti C, Mathes T, van Stokkum IH, Mullen KM, Groot ML, van Grondelle R, Hegemann P, Kennis JT: **Hydrogen bond switching among flavin and amino acid side chains in the BLUF photoreceptor observed by ultrafast infrared spectroscopy**. *Biophysical Journal* 2008, **95**(10);4790-4802.
14. Dragnea V, Waegele M, Balascuta S, Bauer CE, Dragnea B: **Time-resolved spectroscopic studies of the AppA blue-light receptor BLUF domain from Rhodobacter sphaeroides**. *Biochemistry* 2005, **44**(49):15978-15985.
15. Gauden M, Grinstead JS, Laan W, van Stokkum IHM, Avila-Perez M, Toh KC, Boelens R, Kaptein R, van Grondelle R, Hellingwerf KJ *et al*: **On the Role of Aromatic Side Chains in the Photoactivation of BLUF Domains**. *Biochemistry* 2007, **46**(25):7405-7415.
16. Gauden M, van Stokkum IHM, Key JM, L ü hrs DC, van Grondelle R, Hegemann P, Kennis JTM: **Hydrogen-bond switching through a radical pair mechanism in a flavin-binding photoreceptor**. *P Natl Acad Sci USA* 2006, **103**(29):10895-10900.
17. Kennis JTM, Groot ML: **Ultrafast spectroscopy of biological photoreceptors**. *Current Opinion in Structural Biology* 2007, **17**(5):623-630.
18. Toh KC, van Stokkum IHM, Hendriks J, Alexandre MTA, Arents JC, Perez MA, van Grondelle R, Hellingwerf KJ, Kennis JTM: **On the Signaling Mechanism and the Absence of Photoreversibility in the AppA BLUF Domain**. *Biophysical Journal* 2008, **95**(1):312-321.
19. Masuda S, Hasegawa K, Ono TA: **Tryptophan at position 104 is involved in transforming light signal into changes of beta-sheet structure for the signaling state in the BLUF domain of AppA**. *Plant & cell physiology* 2005, **46**(12):1894-1901.
20. Masuda S, Hasegawa K, Ohta H, Ono TA: **Crucial role in light signal transduction for the conserved Met93 of the BLUF protein PixD/Slr1694**. *Plant & cell physiology* 2008, **49**(10):1600-1606.
21. Yuan H, Bauer CE: **PixE promotes dark oligomerization of the BLUF photoreceptor PixD**. *Proc Natl Acad Sci U S A* 2008, **105**(33):11715-11719.
22. Gauden M, Yeremenko S, Laan W, van Stokkum IHM, Ihalainen JA, van Grondelle R, Hellingwerf KJ, Kennis JTM: **Photocycle of the**

flavin-binding photoreceptor AppA, a bacterial transcriptional antirepressor of photosynthesis genes. *Biochemistry* 2005, **44**(10):3653-3662.

23. van Stokkum IHM, Larsen DS, van Grondelle R: **Global and target analysis of time-resolved spectra**. *Biochim Biophys Acta* 2004, **1657**(2-3):82-104.
24. Okajima K, Yoshihara S, Fukushima Y, Geng XX, Katayama M, Higashi S, Watanabe M, Sato S, Tabata S, Shibata Y *et al*: **Biochemical and functional characterization of BLUF-type flavin-binding proteins of two species of cyanobacteria**. *J Biochem* 2005, **137**(6):741-750.
25. Rajagopal S, Key JM, Purcell EB, Boerema DJ, Moffat K: **Purification and initial characterization of a putative blue light-regulated phosphodiesterase from Escherichia coli**. *Photochem Photobiol* 2004, **80**(3):542-547.
26. Gotze J, Saalfran P: **Serine in BLUF Domains Displays Spectral Importance in Computational Models**. *Journal of Photochemistry and Photobiology B: Biology (in press)* 2008.
27. Grinstead JS, Hsu STD, Laan W, Bonvin AMJJ, Hellingwerf KJ, Boelens R, Kaptein R: **The solution structure of the AppA BLUF domain: Insight into the mechanism of light-induced signaling**. *Chembiochem* 2006, **7**(1):187-193.
28. Kraft BJ, Masuda S, Kikuchi J, Dragnea V, Tollin G, Zaleski JM, Bauer CE: **Spectroscopic and mutational analysis of the blue-light photoreceptor AppA: a novel photocycle involving flavin stacking with an aromatic amino acid**. *Biochemistry* 2003, **42**(22):6726-6734.
29. Zirak P, Penzkofer A, Lehmpfuhl C, Mathes T, Hegemann P: **Absorption and emission spectroscopic characterization of blue-light receptor Slr1694 from Synechocystis sp. PCC6803**. *J Photochem Photobiol B* 2007, **86**(1):22-34.
30. Mullen KM, van Stokkum IHM: **TIMP: An R package for modeling multi-way spectroscopic measurements**. *Journal of Statistical Software* 2007, **18**(3).
31. Laan W, Gauden M, Yeremenko S, van Grondelle R, Kennis JTM, Hellingwerf KJ: **On the mechanism of activation of the BLUF domain of AppA**. *Biochemistry* 2006, **45**(1):51-60.
32. Stanley RJ, Siddiqui MS: **A Stark Spectroscopic Study of N(3)-Methyl, N(10)-Isobutyl-7,8-Dimethylisoalloxazine in Nonpolar Low-Temperature Glasses: Experiment and Comparison with Calculations**. *Journal of Physical Chemistry A* 2001, **105**(49):11001-11008.

33. Kennis JTM, Crosson S, Gauden M, van Stokkum IHM, Moffat K, van Grondelle R: **Primary reactions of the LOV2 domain of phototropin, a plant blue-light photoreceptor**. *Biochemistry* 2003, **42**(12):3385-3392.
34. Sadeghian K, Bocola M, Schutz M: **A conclusive mechanism of the photoinduced reaction cascade in blue light using flavin photoreceptors**. *J Am Chem Soc* 2008, **130**(37):12501-12513.
35. Miura R: **Versatility and specificity in flavoenzymes: control mechanisms of flavin reactivity**. *Chem Rec* 2001, **1**(3):183-194.
36. Müller F, Brüstlein M, Hemmerich P, Massey V, Walker WH: **Light-Absorption Studies on Neutral Flavin Radicals**. *European Journal of Biochemistry* 1972, **25**(3):573-580.
37. Kottke T, Heberle J, Hehn D, Dick B, Hegemann P: **Phot-LOV1: Photocycle of a blue-light receptor domain from the green alga Chlamydomonas reinhardtii**. *Biophysical Journal* 2003, **84**(2):1192-1201.
38. Swartz TE, Corchnoy SB, Christie JM, Lewis JW, Szundi I, Briggs WR, Bogomolni RA: **The photocycle of a flavin-binding domain of the blue light photoreceptor phototropin**. *Journal of Biological Chemistry* 2001, **276**(39):36493-36500.
39. Schwede T, Kopp J, Guex N, Peitsch MC: **SWISS-MODEL: An automated protein homology-modeling server**. *Nucleic acids research* 2003, **31**(13):3381-3385.
40. Zirak P, Penzkofer A, Schiereis T, Hegemann P, Jung A, Schlichting I: **Absorption and fluorescence spectroscopic characterization of BLUF domain of AppA from *Rhodobacter sphaeroides*** *Chemical Physics* 2005, **315**(1-2):142-154.
41. Borucki B, Otto H, Joshi CP, Gasperi C, Cusanovich MA, Devanathan S, Tollin G, Heyn MP: **pH Dependence of the photocycle kinetics of the E46Q mutant of photoactive yellow protein: protonation equilibrium between I1 and I2 intermediates, chromophore deprotonation by hydroxyl uptake, and protonation relaxation of the dark state**. *Biochemistry* 2003, **42**(29):8780-8790.
42. Hendriks J, van Stokkum IHM, Hellingwerf KJ: **Deuterium Isotope Effects in the Photocycle Transitions of the Photoactive Yellow Protein**. *Biophysical Journal* 2003, **84**(2):1180-1191.
43. Novoderezhkin VI, Yakovlev AG, vanGrondelle R, Shuvalov VA: **Coherent Nuclear and Electronic Dynamics in Primary Charge Separation in Photosynthetic Reaction Centers: A Redfield Theory Approach**. *Journal of Physical Chemistry B* 2004, **108**(22):7445-7457.
44. Shuvalov VA, Yakovlev AG: **Coupling of nuclear wavepacket motion**

and charge separation in bacterial reaction centers. *FEBS Lett* 2003, **540**(1-3):26-34.

45. Solar S, Getoff N, Surdhar PS, Armstrong DA, Singh A: **Oxidation of Tryptophan and N-Methylindole by N3., Br2-, and (Scn)2- Radicals in Light-Water and Heavy-Water Solutions - a Pulse-Radiolysis Study**. *Journal of Physical Chemistry* 1991, **95**(9):3639-3643.
46. Aubert C, Vos MH, Mathis P, Eker APM, Brettel K: **Intraprotein radical transfer during photoactivation of DNA photolyase (vol 405, pg 586, 2000)**. *Nature* 2000, **407**(6806):926-926.
47. Bent DV, Hayon E: **Excited state chemistry of aromatic amino acids and related peptides. III. Tryptophan**. *Journal of the American Chemical Society* 1975, **97**(10):2612-2619.
48. Harriman A: **Further comments on the redox potentials of tryptophan and tyrosine**. *Journal of Physical Chemistry* 1987, **91**(24):6102-6104.
49. Domratcheva T, Grigorenko BL, Schlichting I, Nemukhin AV: **Molecular models predict light-induced glutamine tautomerization in BLUF photoreceptors**. *Biophys J* 2008, **94**(10):3872-3879.
50. Neiss C, Saalfrank P, Parac M, Grimme S: **Quantum Chemical Calculation of Excited States of Flavin-Related Molecules**. *Journal of Physical Chemistry A* 2003, **107**(1):140-147.
51. Alexandre MT, van Grondelle R, Hellingwerf KJ, Robert B, Kennis JT: **Perturbation of the ground-state electronic structure of FMN by the conserved cysteine in phototropin LOV2 domains**. *Phys Chem Chem Phys* 2008, **10**(44):6693-6702.

Appendix

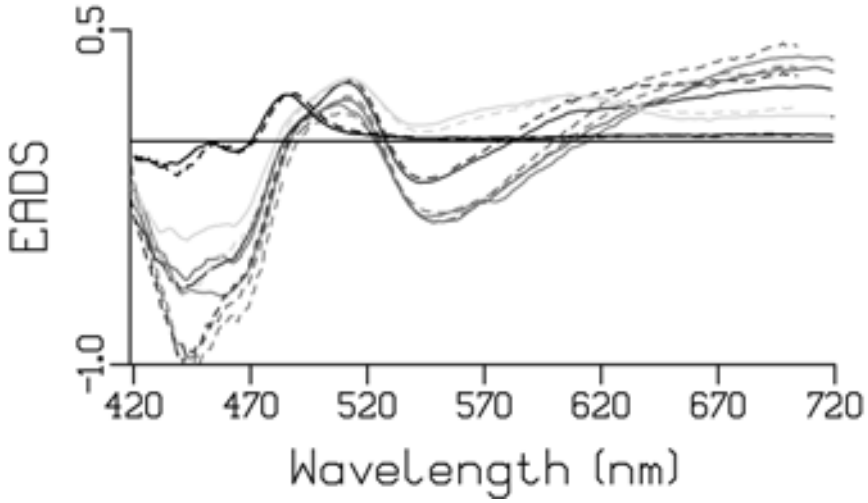

FIGURE A: Evolution-Associated Difference Spectra that follow from a global analysis of transient absorption data on the wild type Slr1694 BLUF domain from Synechocystis PCC6803 in H2O buffer, this work (dashed lines) and in Gauden *et al* [1] (solid lines). The excitation wavelength was 400 nm. The datasets were simultaneously analyzed, with resulting time constants of 0.9 ps (gray), 3.4 ps (gray), 17 ps (dark gray), 108 ps (light gray) and a non-decaying component (black). The spectra were normalized at 550 nm (maximum intensity for the flavin stimulated emission). The EADS of the two datasets deviate on the blue side (flavin bleaching between 420 and 486 nm) and on the red side of the spectra (flavin singlet excited state absorption between ~600 and 700 nm), which probably arises from slightly different spectrospatial overlaps of pump and probe beams.

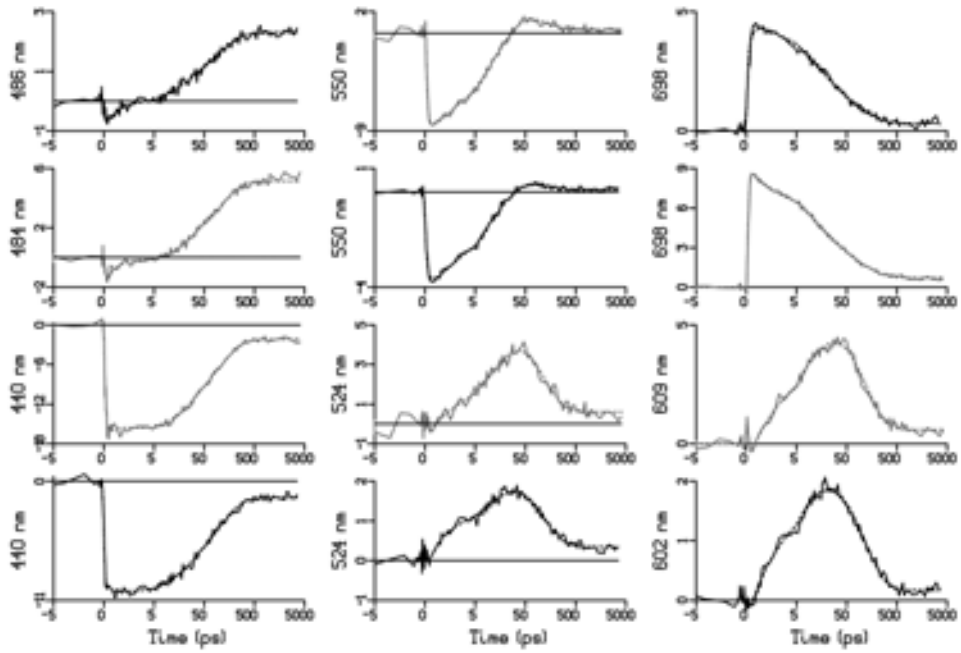

FIGURE B: Kinetic traces at selected wavelengths for wild type Slr1694 presented in Gauden *et al* [1] (black lines) and in this work (gray lines). The temporal evolution between the datasets is essentially identical.

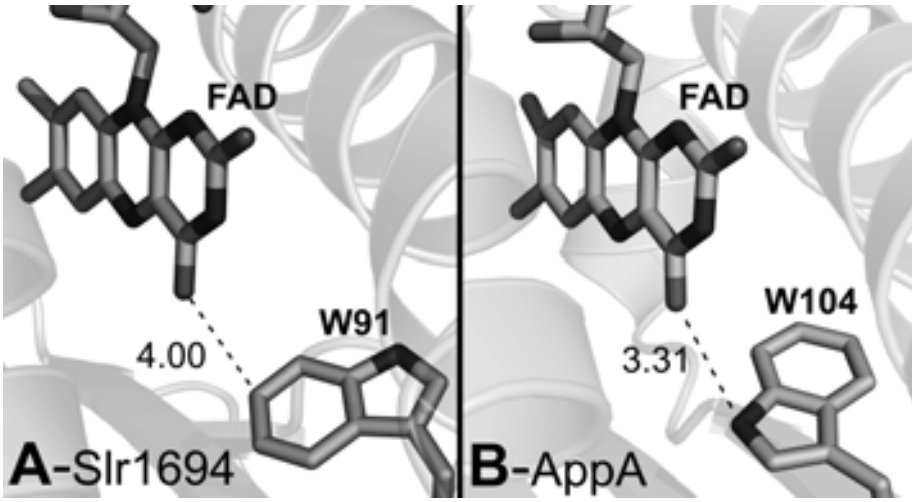

FIGURE C: Close up of the FAD binding pocket in the BLUF crystal structures: (A), W91 and FAD in Slr1694 [2]; (B) W104 and FAD in AppA [3].

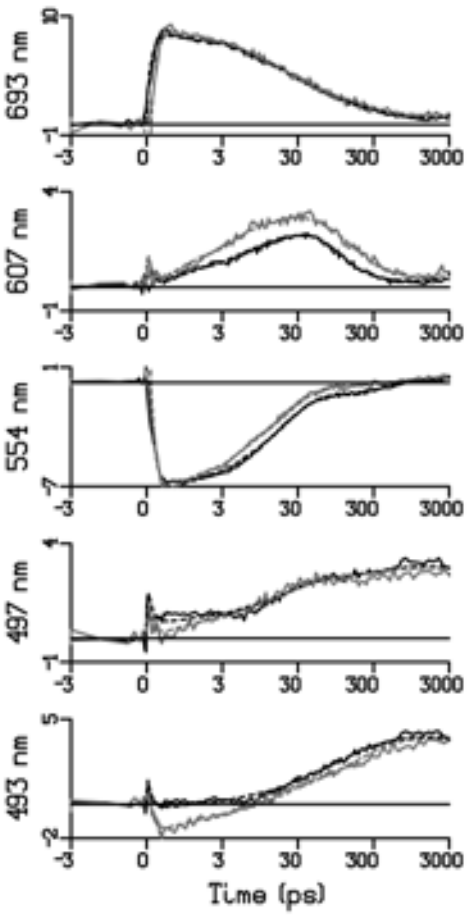

FIGURE D: Kinetic traces at selected wavelengths for the Synechocystis Slr1694 W91F mutant in H_2O and D_2O (black and red lines, respectively). The excitation wavelength was 400 nm. The fit using e target analysis is shown as a dashed line. Note that the time axis is linear from -3 to 3 ps, and logarithmic thereafter. The selected wavelengths correspond to: 493 nm, maximum of signaling state induced absorption; 497 nm, first isosbestic point of FAD*; 554 nm, maximum of the FAD stimulated emission; 607 nm, second isosbestic point of FAD*; 693 nm, FAD singlet excited state absorption.

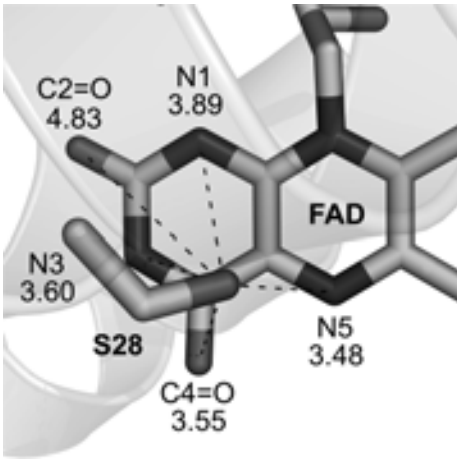

FIGURE E: Close up of the FAD binding pocket in the Slr1694 crystal structure [2]: FAD and S28.

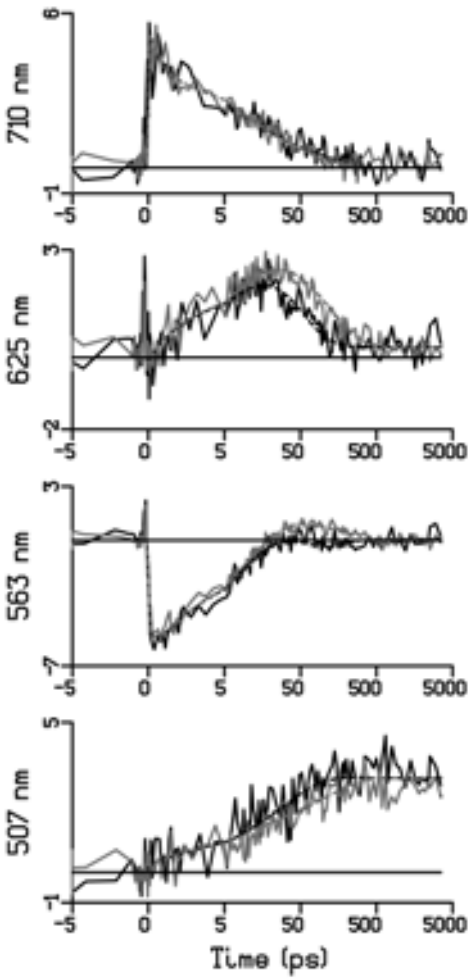

FIGURE F: Selected kinetic traces for the Synechocystis Slr1694 S28A mutant in H_2O and D_2O (black and gray lines, respectively). The excitation wavelength was 400 nm. The fit using target analysis is shown as a dashed line. Note that the time axis is linear from −5 to 5 ps, and logarithmic thereafter. The chosen wavelengths correspond to: 507 nm, maximum of signaling state induced absorption; 563 nm, maximum of the FAD stimulated emission; 625 nm, isosbestic point of FAD*; 710 nm, flavin singlet excited state absorption.

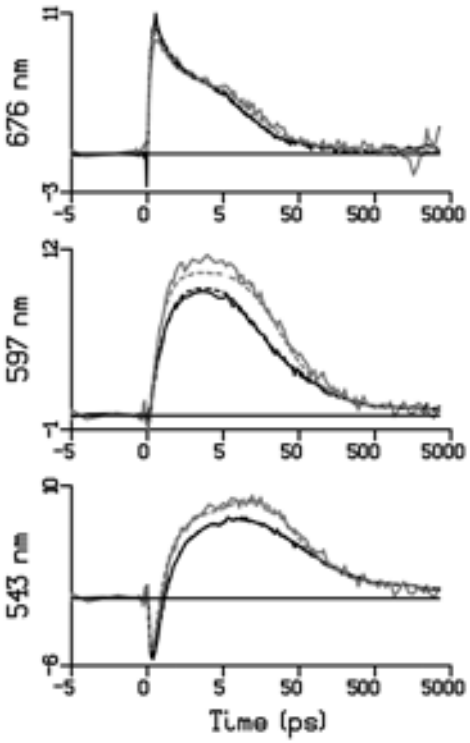

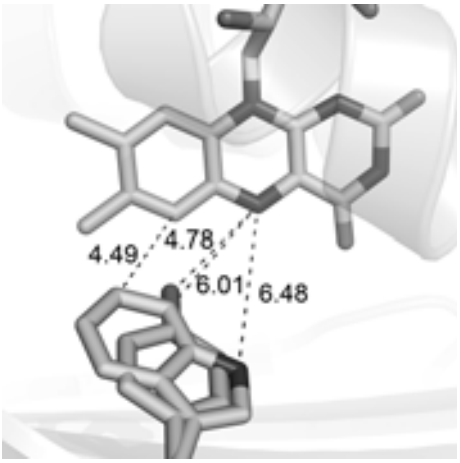

FIGURE H: Close up of the FAD binding pocket in the Slr1694 crystal structure [2] FAD and Y8 and homology-modeled W8 .

FIGURE G: Selected kinetic traces for Synechocystis Slr1694 Y8W mutant in H_2O and D_2O (black and gray lines, respectively). The excitation wavelength was 400 nm. The fit using target analysis is shown as a dashed line. Note that the time axis is linear from -5 to 5 ps, and logarithmic thereafter. The chosen wavelengths correspond to: 543 nm, maximum of the flavin stimulated emission; 597 nm, second isosbestic point; 676 nm, flavin singlet excited state absorption.

Appendix: References

1. Gauden M, van Stokkum IHM, Key JM, L ü hrs DC, van Grondelle R, Hegemann P, Kennis JTM: **Hydrogen-bond switching through a radical pair mechanism in a flavin-binding photoreceptor**. *P Natl Acad Sci USA* 2006, **103**(29):10895-10900.
2. Yuan H, Anderson S, Masuda S, Dragnea V, Moffat K, Bauer CE: **Crystal structures of the Synechocystis photoreceptor Slr1694 reveal distinct structural states related to signaling**. *Biochemistry* 2006, **45**(42):12687-12694.
3. Anderson S, Dragnea V, Masuda S, Ybe J, Moffat K, E.Bauer C: **Structure of a novel photoreceptor, the BLUF domain of AppA from Rhodobacter sphaeroides**. *Biochemistry* 2005, **44**(22):7998-8005.